

# Lawrence Berkeley National Laboratory

## LBL Publications

### Title

Experimental validation and model development for thermal transmittances of porous window screens and horizontal louvred blind systems

### Permalink

<https://escholarship.org/uc/item/5f791782>

### Journal

Journal of Building Performance Simulation, 11(2)

### ISSN

1940-1493

### Authors

Hart, Robert  
Goudey, Howdy  
Curcija, D Charlie

### Publication Date

2018-03-04

### DOI

10.1080/19401493.2017.1323010

Peer reviewed



# Lawrence Berkeley National Laboratory

## Experimental Validation and Model Development for Thermal Transmittances of Porous Window Screens and Horizontal Louvered Blind Systems

Robert Hart, Howdy Goudey, D. Charlie Curcija

Energy Technologies Area

May 2017



## **Disclaimer**

This document was prepared as an account of work sponsored by the United States Government. While this document is believed to contain correct information, neither the United States Government nor any agency thereof, nor the Regents of the University of California, nor any of their employees, makes any warranty, express or implied, or assumes any legal responsibility for the accuracy, completeness, or usefulness of any information, apparatus, product, or process disclosed, or represents that its use would not infringe privately owned rights. Reference herein to any specific commercial product, process, or service by its trade name, trademark, manufacturer, or otherwise, does not necessarily constitute or imply its endorsement, recommendation, or favoring by the United States Government or any agency thereof, or the Regents of the University of California. The views and opinions of authors expressed herein do not necessarily state or reflect those of the United States Government or any agency thereof or the Regents of the University of California.

## **Acknowledgments**

This work was supported by the Assistant Secretary for Energy Efficiency and Renewable Energy, Building Technologies Office, of the U.S. Department of Energy under Contract No. DE-AC02-05CH11231.

# **Experimental Validation and Model Development for Thermal Transmittances of Porous Window Screens and Horizontal Louvered Blind Systems**

Robert Hart, Howdy Goudey, D. Charlie Curcija  
*Lawrence Berkeley National Laboratory, Berkeley, CA USA*

Virtually every home in the U.S. has some form of shades, blinds, drapes or other window attachment, but few have been designed for energy savings. In order to provide a common basis of comparison for thermal performance it is important to have validated simulation tools. This paper outlines a review and validation of the ISO 15099 center-of-glass thermal transmittance correlations for naturally ventilated cavities through measurement and detailed simulations. The focus is on the impacts of room-side ventilated cavities, such as those found with solar screens and horizontal louvered blinds. The thermal transmittance of these systems is measured experimentally, simulated using CFD analysis, and simulated utilizing simplified correlations from ISO 15099. Correlation coefficients are proposed for the ISO 15099 algorithm that reduce the mean error between measured and simulated heat flux for typical solar screens from 16% to 3.5% and from 13% to 1% for horizontal blinds.

Keywords: building energy; windows; window attachment; shading; U-factor; heat transfer

## **Introduction**

Virtually every home in the U.S. has some form of shades, blinds, drapes or other window attachment, but few have been designed for energy savings. High performance solutions for residential and commercial window attachments therefore offer large short-term energy savings potential. Due to the wide variety of window attachment solutions, energy savings can be accomplished in all climates by utilizing systems that reduce heating energy, reduce cooling energy, or both. These products can also reduce mechanical heating and/or cooling system sizing and improve indoor thermal comfort. Some high performance products are available today but more rapid market adoption would be facilitated by better optimization and selection criteria, e.g. fair performance comparison and rating labels. There are also opportunities to re-engineer and enhance existing products to dramatically improve their performance, both in terms of intrinsic properties and in operations. It is important to have validated simulation tools to provide a common basis of comparison for window attachments. Simulation tools allow manufacturers to efficiently design more cost effective high performance products through the use of parametric analysis and optimization.

Several different approaches to simulate windows with attachments have been studied and developed. The primary focus of these works has been the experimental measurement, simulation, and simplified model development of solar heat gain for horizontal louvered blinds (venetian blinds) located between-glass and room-side. Existing experimental work includes Clark et al. (2013), Collins and Harrison (2004a), Cuevas et al. (2010), Fang (2000), Garnet et al. (1995), Naylor et al. (2002a), and Naylor et al. (2002b). Simulation and simplified model development is included in the work of Ye et al. (1999), Laouadi (2009), Naylor and Shahid (2006), Marjanovic et al. (2005), Oosthuizen et al. (2005), Roelevelld et al. (2010), Shahid and Naylor (2005), Collins (2004), and Wright (2008). Additional work involving SHGC of blinds under solar load has been done by Collins and Harrison (1999, 2004b), Harrison and van Wonderen (1998), Kotey et al. (2009), and Tait (2006). Finally, blinds between glass have been studied by Collins et al. (2009), Naylor and Collins (2005), and Wright et al. (2008). Ventilated glazing, or air-flow windows, can be representative of in-plane shading systems. Experiments and model development has been done for these windows, but primarily with forced, rather than natural ventilation by Carlos and Corvacho (2011, 2014), Tanimoto and Kimura (1997), and Ismail and Henríquez (2005).

Relatively little research has been done to characterize the night-time (zero solar load) U-factor impacts of attachment products other than venetian blinds, including in-plane products such as solar screens, roller shades, cellular shades, insect screens, and drapes. Existing experimental work includes guarded head plate measurements of room-side and between-glass solar screens made by Grasso et al. (1979, 1990), Fang (2001), Wang et al. (2015)], Kotey et al. (2009), Cuevas et al. (2010), and insect screens by Kotey et al. (2009), Brunger et al. (1999), and Norris (2009). Simulation and simplified model development of these products is even less extensive but Fang, Wang et al., and Kotey et al. do include simplified model development along with their experimental work.

The thermal performance of in-plane products can be modelled similar to sealed (insulating) glazing with modifications to account for long-wave (IR) radiant transmission, gas flow across attachments layers, and shape factors affecting convection over the surface. Wright (2008) developed a resistance network model and van Dijk and Oversloot (2003) developed a model utilizing buoyancy driven pressure difference modifications to the surface convection coefficient of sealed cavities to account for gas flow across layers. The van Dijk model is utilized in ISO 15099 (2003) and the WIS (van Dijk 2003) and WINDOW (Tarcog 2006) simulation programs. NF EN 13125 standard (2012) is an alternative model that defines additional thermal resistance over base glazing provided by shutters and blinds based on the perimeter and surface openness.

The ISO 15099 ventilated window model determines surface convection coefficients based on the opening characteristics of layers adjacent to ventilated cavities. The model divides layer openings into four distinct categories; top, bottom, sides, and surface (front), as shown in Figure 1. While these equations are physically based, the standard does not cite any validation of the approach through either measurements or detailed numerical simulation. Additionally, the model presented in ISO 15099 for simulation of slat type shading devices is incomplete. For these products it calls for the determination of an equivalent surface openness based on measurement or CFD simulation.

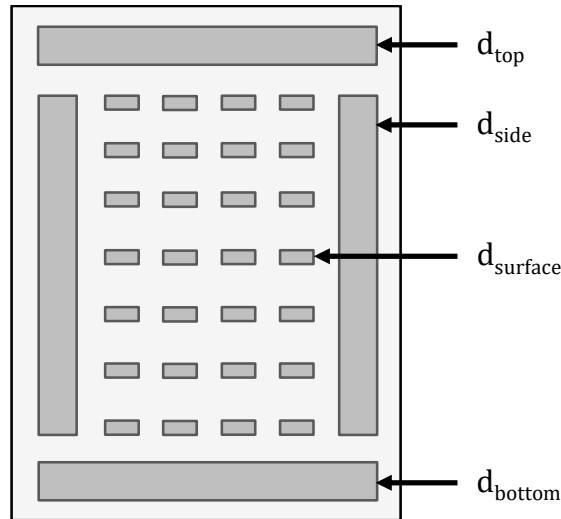


Figure 1. Illustration of ISO 15099 ventilated shade layer opening locations.

Surface openness of shade systems,  $d_{surface}$  in Figure 1, has primarily been studied for highly porous surfaces such as insect screens by Kotey et al. (2009), Brunger et al. (2009), and Norris (2009). Model development based on experimental analysis for pressure drop and fluid flow through low to medium porosity screens has been done by Miguel (1998) based on the Darcy-Forchheimer Law. Typical solar screens used in window systems range from low  $d_{surface} \cong 0.01$  to medium  $d_{surface} \cong 0.10$ . Horizontal blind products typically have very high  $d_{surface} \cong .99$  when slats are horizontal and greater than  $d_{surface} \cong .70$  percent when fully tilted. For porous screens and horizontal blind products with a natural convection boundary condition typical of room-side mount shades, Laouadi (2009) proposed a model based on penetrative convection in porous media, from Bejan (2004). The proposed models from Laouadi, Wright (2008), and others are founded on an adjustment of the glass-to-shade cavity depth,  $d_{gap}$ , as a function of slat width, pitch, and/or openness.

The work presented in this report is a review, validation and proposed revision to the ISO 15099 center-of-glass (COG) heat transfer correlations optimized for naturally ventilated cavities. The focus is on impacts to system thermal transmittance due to variations in surface openness from room-side mounted screens and louvered horizontal (venetian) blinds. Thermal transmittance is measured experimentally and simulated utilizing existing correlations from ISO 15099. Revised correlation coefficients to the ISO algorithm are proposed to better correlate simulation with experimental results.

## Simulation Methodology

The LBNL developed simulation program, WINDOW, calculates heat transfer through glazing assemblies based on one-dimensional correlations of average values. The correlations were developed through a variety of means including laboratory measurements, detailed simulations, and analytical models. The correlations and their sources are defined in ISO 15099. Of specific interest for this work is the model presented for thermally driven ventilation. The model is based on introducing a modifier to the unvented correlation to determine an adjusted average surface-to-air heat transfer coefficient for the cavity between glass and shade layers. The modifying equations are physically based and incorporate several pressure drop principles for air through a channel

including Bernouilli, Hagen-Poiseuille, and entrance/exit correlations.

The inlet and outlet pressure loss of a cavity open to the indoor room,  $\Delta P_z$ , is calculated with Equations 1-5, where the use of in/out and top/bot are dependent on the direction of flow, as determined by the glass surface temperature relative to the indoor temperature.

$$\Delta P_z = 0.5\rho v^2(Z_{in} + Z_{out}) \quad (1)$$

$$Z_{in/out} = \left( \frac{A_s}{0.6A_{eq,in/out}} - 1 \right)^2 \quad (2)$$

$$A_{eq,in/out} = A_{top/bot} + \frac{1}{2} \frac{A_{bot/top}}{A_{bot} + A_{top}} (A_l + A_r + A_h) \quad (3)$$

$$A_h = d_{surface} \cdot W \cdot H \quad (4)$$

$$A_s = d_{gap} \cdot W \quad (5)$$

$\rho$  is the fluid density,  $v$  is the fluid velocity,  $Z_{in/out}$  is the pressure loss factor of the cavity,  $A_s$  is the cross-section area of the cavity,  $d_{gap}$  is the glass-to-shade cavity depth,  $d_{surface}$  is the openness fraction (0 - 1),  $W$  is the window width,  $H$  is the window height,  $A_{eq}$ , is the equivalent inlet/outlet area of the cavity, and  $A_l, A_r, A_{top}, A_{bot}, A_h$  are the areas of the left, right, top, bottom, and front surface ventilation gaps respectively.

The set of equations 1 through 5 include an inherent minimum of pressure loss coefficient,  $Z$ , when the calculated inlet or outlet area,  $A_{eq}$ , equals 5/3 the cross section area,  $A_s$ . This limits the validity of the model to  $A_{eq}$  less than 5/3 of  $A_s$ . Figure 2b illustrates this minimum with a surface map of calculated  $Z$  values ( $\log(Z)$  plotted to show contours) over a range of  $A_{eq}$  based on a 1m x 1m window. Figure 2a shows a slice of the surface plot at a typical  $d_{gap} = 15$  mm. Window surface area,  $A_w$ , is typically one to two orders of magnitude larger than the cross-section area,  $A_s$ . This means that  $A_{eq}$  exceeds  $A_s$  at relatively low surface openness. For a typical glass-to-shade gap,  $d_{gap} = 15$ mm, the local minimum in  $Z$ , and in turn valid openness range of the algorithm, occurs at an openness of  $d_{surface} \cong 0.1$ .

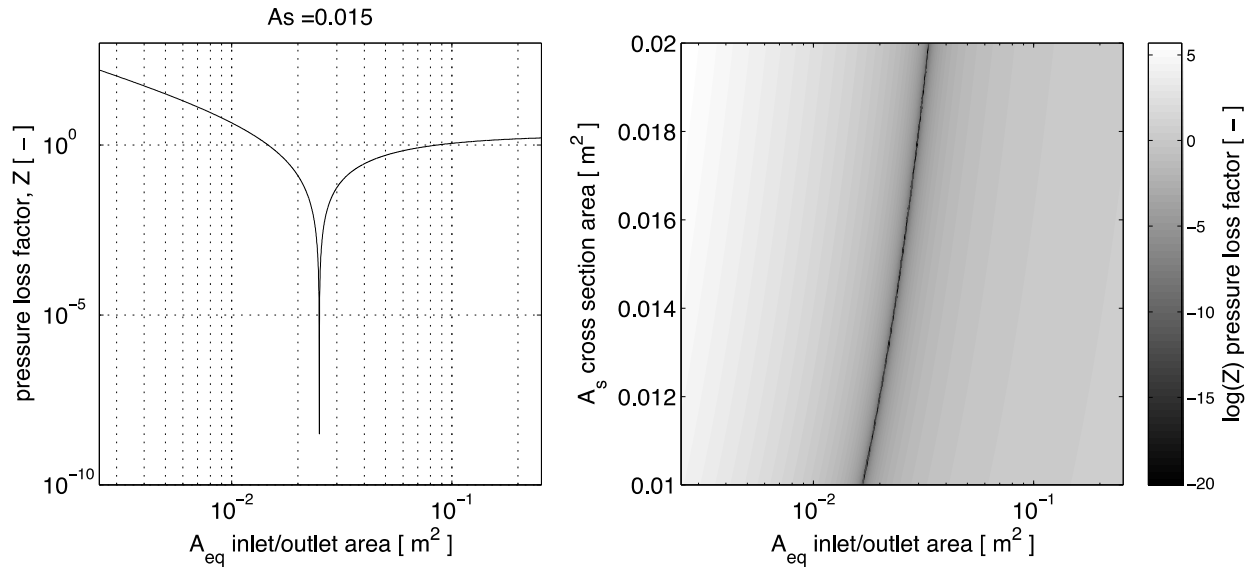


Figure 2. (a) Pressure loss factor,  $Z$ , as a function of  $A_{eq}$  at  $A_s = 0.015\text{m}^2$ ; and (b) surface plot of  $Z$  as a function of  $A_s$  and  $A_{eq}$  for a 1m x 1m window. The minimum follows the predicted ratio of 5/3 between  $A_{eq}$  and  $A_s$ .

The inlet and outlet pressure loss examined above is combined with additional pressure loss models to determine total layer flow resistance. The velocity of the fluid exiting the cavity is then calculated, leading to the revised surface convection coefficient by Equation 6,

$$h_{cv} = h_c + 2v \quad (6)$$

$$h_c = \frac{Nu \cdot k_{air}}{d_{gap}} \quad (7)$$

where  $h_c$  is the un-vented gap surface-to-surface convection coefficient,  $h_{cv}$  is the ventilated gap surface-to-air convection coefficient,  $k_{air}$  is thermal conductivity of air at the mean cavity temperature, and the Nusselt number ( $Nu$ ) is the ratio of convective to conductive heat transfer across the cavity. Multiple empirical correlations controlled by the cavity height-to-width aspect ratio ( $AR$ ) and  $Ra$  ranges are used for  $Nu$  in ISO 15099.

Models and experimental analysis of pressure drop for flow through perforated surfaces has been extensively studied. The Darcy-Forchheimer Law (Equation 8) is the relation used to describe velocity of a steady moving flow ( $Re > 1$ ) under a pressure gradient, where Reynolds number ( $Re$ ) is the ratio of inertial forces to viscous forces in a moving fluid. The linear term accounts for the momentum transfer from fluid to surface while the non-linear term accounts for the inertia effects,

$$\frac{\mu}{K} v + \rho \frac{Y}{K^{1/2}} v^2 = \frac{\partial p}{\partial x} \quad (8)$$

where  $\rho$  is the fluid density,  $\mu$  is the dynamic viscosity,  $v$  is the velocity,  $p$  is the pressure,  $x$  is the direction vector of the pressure gradient,  $K$  is the permeability, and  $Y$  is the inertial factor (dependent on pore characteristics). Miguel (1998) correlated  $K$  and  $Y$  to a logarithmic model of the form shown in Equation 9 based on experimental analysis.

$$P = a \cdot d_{surface}^b \quad (9)$$

$P$  represents the correlation constant  $K$  or  $Y$  and  $a$  &  $b$  are constants determined by regression analysis from measurements of perforated screen materials. Miguel showed that the shape of yarns and mesh geometry have negligible impact on airflow characteristics through screens, which allows the model to be dependent solely on  $d_{surface}$  and thickness of the layer.

## Experimental Methodology

Screen openness is typically reported by manufacturers based on the calculated average geometrical openness using thread diameter and threads per inch of the weave. The openness of louvered blinds is not reported since the majority of slats are solid and the overall layer openness is dependent on slat angle. Two methods are used to verify manufacturer reported openness. The optical method is performed with a spectrometer where the openness is equivalent to the visible specular transmittance of the material. The specular transmittance is calculated by measurement of direct-hemispherical and direct-diffuse transmittance using an integrating sphere. The measured



value includes two components: light transmitted through openings without fabric interaction, and light forward scattered at an outgoing angle of less than 5 degrees. The scattered light could be due to any combination of surface reflections and light scattered after traveling through the threads (for translucent materials). The flow method, ASTM D737, is performed by measuring volumetric airflow ( $\text{cm}^3 \text{ s}^{-1}$ ) through a set sample area ( $\text{cm}^2$ ) at a set pressure drop of 125 Pa (ASTM 2008).

The emissivity of screen layers and blind slats are directly measured according to ASTM C 1371-15, Standard Test Method for Determination of Emittance On Material Near Room Temperature Using Portable Emisimeters (ASTM 2015). If the sample is not opaque it is possible to get both the transmittance and emissivity through measurement of the sample on two different opaque backing surfaces (Devices 1981). The measured emittance,  $E_a$ , in each case is given by equation 10.

$$E_a = E_s + T_s \left( 1 - T_s \frac{1 - E_b}{1 - (1 - E_s - T_s)(1 - E_b)} \right) \quad (10)$$

where E represents emittance, T transmittance, index s denotes sample, and b backing material. By doing this for two known backing materials with a large difference, the system of two equations can be used to solve for  $T_s$  and  $E_s$ . No simple closed solution to the system of two equations exists, so an iterative solution needs to be applied.

Industry standard quantitative measurement of window heat flow is performed with calorimetric “hot box” instruments as outlined in ISO 12567 (ISO 2010). An alternative method utilizing calibration transfer standards (CTS) (ASTM 2014) is used for the current work. Figure 3 illustrates the test chamber configuration.

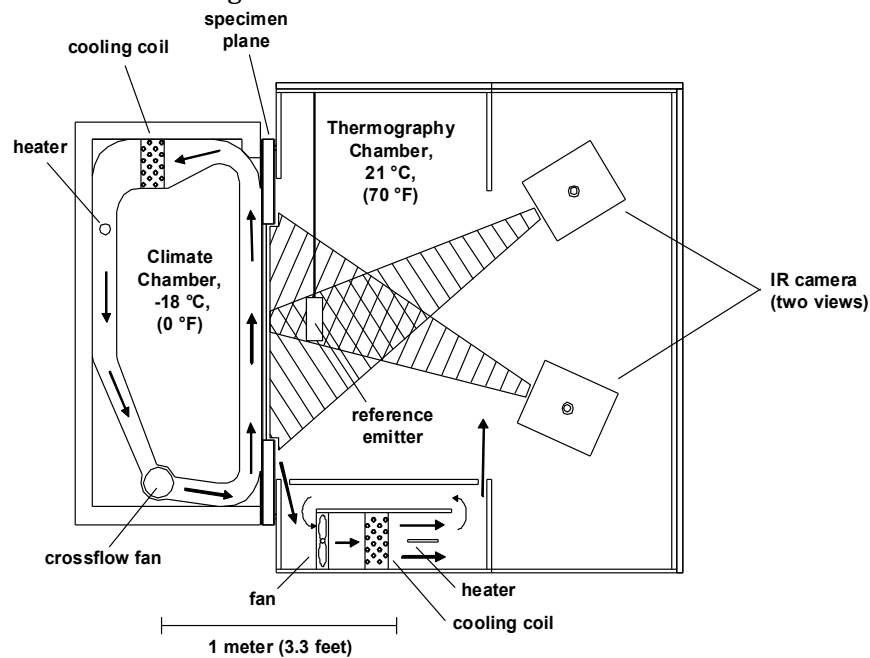


Figure 3. Schematic cross-section of environmental test chambers

The CTS represents typical thermal resistance of a double-pane clear glazing system. Thermocouples are placed in a 3 x 6 grid (18 per surface) on the inside surface of two 1080 mm by 775 mm glass panes with a calibrated foam layer between. The calibrated system thermal resistance with many temperature pair measurements allows for calculation of local heat flow through the specimen in many locations. Illustrations of configurations with the CTS specimen along with a sample shade and inside mount horizontal blinds are shown in Figures 4 and 5

respectively. An outside mount blind configuration is also illustrated in Figure 5 for clarity of the mounting type.

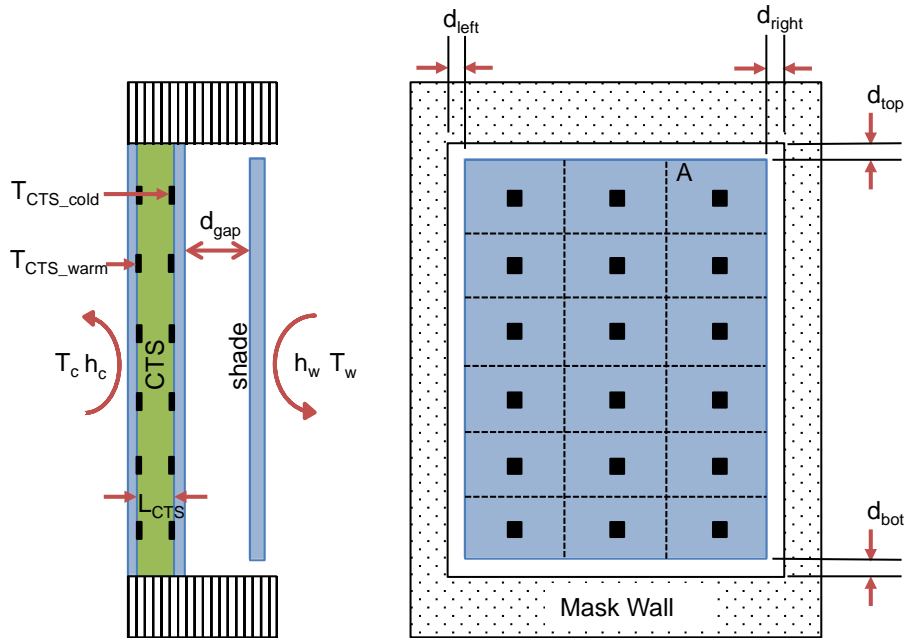


Figure 4. Side and front views of the CTS and screen assembly within specimen mounting plane of the thermal test chamber

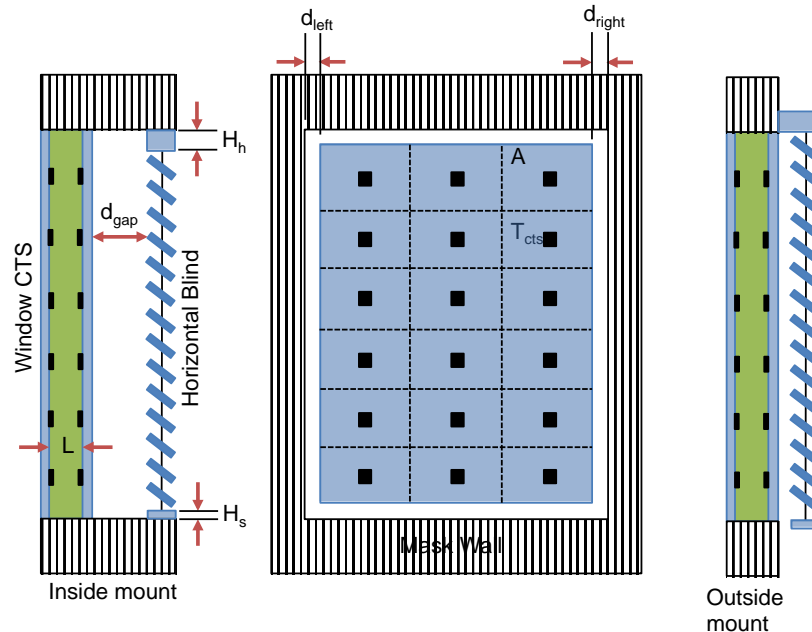


Figure 5. Illustration of the CTS and horizontal blind assembly within specimen mounting plane of the thermal test chamber. Measurements conducted with inside mount configuration.

Equations 11 and 12 determine heat flow through the CTS and shade, with the calculated thermal conductivity of the CTS foam,  $k_{CTS}$ , foam thickness,  $L_{CTS}$ , and measured temperatures,

$T_{CTS\_cold/warm}$ , on either side of the CTS. All derived performance characteristics (such as heat flow and surface coefficients) are calculated for each grid area,  $A$ , and then summed over the entire specimen area to determine the overall performance of the system. Heat flux,  $q$ , is then calculated by dividing by the total specimen surface area.

$$Q = k_{CTS}/L_{CTS} \Sigma A(T_{CTS\_warm} - T_{CTS\_cold}) \quad (11)$$

$$q = Q/A \quad (12)$$

### ***Boundary conditions***

The ISO 15099 flat plate correlations for natural convective surface-to-air heat-transfer coefficient on vertical surfaces are utilized to determine room side convection in this work. Forced convection on the cold side is very complicated to characterize since the as-tested geometry is somewhat complex, the flow is turbulent, and the uniformity of fan flow in the experiment is unpredictable. The most accurate match of simulation to the measured conditions is therefore achieved by assigning an area-weighted average of the measured local combined surface heat-transfer coefficient in the simplified model.

The cold side surface heat-transfer coefficient is sufficiently large that its resistance is small compared to the overall system resistance. The resistance cannot be neglected but small deviations in the assigned numerical coefficient from the as-tested conditions have minor impact to the simulated overall system performance. A summary of boundary conditions is presented below. These boundary conditions are the set points for experiments and are therefore nominal values. The actual measured values are used as inputs for the simulations.

- Warm side:  $T_w = 21 \text{ }^\circ\text{C}$   
     Radiation coefficient - surface to ambient temperature ( $T_w$ )  
     Convection coefficient – ISO 15099 flat plate model
- Cold side:  $T_c = -18 \text{ }^\circ\text{C}, -9 \text{ }^\circ\text{C}, \text{ or } 0 \text{ }^\circ\text{C}$   
     Combined radiation and convection to ambient temperature ( $T_c$ )

### ***Fabrics and Shade Materials with Porosity***

Five parameters are investigated in depth for perforated surface scenarios; screen surface openness, inside-outside temperature differential, shade-window gap depth, and left and right gap width. The ranges of these parameters are listed in Table 1. A total of 40 different combinations of the five parameters are measured and simulated using the simplified simulation model.

Table 1. Measurement parameters for side gap investigation

<b>Variable</b>	<b>Parameter</b>	<b>Set points</b>	<b>Unit</b>
$d_{\text{surface}}$	surface openness	Table 2	-

$T_c$	cold side Temperature	0, -18	°C
$d_{gap}$	shade-window gap depth	17.8, 46.4	mm
$d_{left}$	left gap width	0, 12.7	mm
$d_{right}$	right gap width	0, 12.7	mm
$d_{top}$	top gap width	0	mm
$d_{bot}$	bottom gap width	0	mm

### Horizontal Louvered Blinds

Fifteen different horizontal blind products that represent the range of currently available products on the market are examined. Seven parameters are investigated in depth; slat width, pitch, rise, conductivity, tilt angle, inside-outside temperature differential, slat-window gap width, and left and right gap dimensions. The ranges of these parameters are listed in Tables 2 and 3 and the geometry is defined in Figures 5 and 6. A total of 176 different combinations of the seven parameters are measured and simulated using the WINDOW simulation model.

Table 2. Measurement parameters for horizontal blind investigation

Variable	Parameter	Set points	Unit
w	slat width	Table 2	mm
p	pitch	Table 2	mm
r	rise	Table 2	mm
$k_s$	conductivity	Table 2	$W m^{-1} K^{-1}$
$T_c$	cold side temperature	-18, -9, 0	°C
$d_{left}, d_{right}$	side gap width	0, 12.7	mm
$\phi$	tilt angle	~80,45,0, -45,~-80	deg

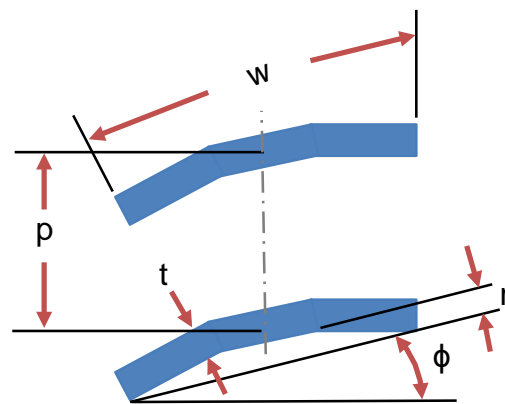


Figure 6. Horizontal blind slat geometry

Table 3. Horizontal blind properties

ID	slat width w [mm]	pitch p [mm]	thickness t [mm]	rise r [mm]	head height H <sub>h</sub> [mm]	sill height H <sub>s</sub> [mm]	material emissivity e [-]	conductivity k <sub>s</sub> [Wm <sup>-1</sup> K <sup>-1</sup> ]
HB01	63.5	54.0	2.8	0	38.1	15.6	0.90	0.17
HB02	50.8	44.2	3.2	0	38.1	15.6	0.90	0.17
HB03	63.5	53.3	2.9	3.7	38.1	16.9	0.90	0.17
HB04	50.8	43.8	0.3	3.2	38.1	15.2	0.82	160
HB05	25.4	21.0	3.2	0	25.4	16.5	0.90	0.14
HB06	50.8	43.8	3.2	0	38.1	15.9	0.90	0.14
HB07	60.3	53.0	3.2	0	38.1	15.9	0.90	0.14
HB08	12.7	12.1	0.3	0.8	25.4	10.2	0.82	160
HB09	25.4	19.4	0.3	1.5	25.4	10.8	0.82	160
HB10	12.7	11.6	0.3	1.3	36.1	11.9	0.73	160
HB11	50.8	41.3	0.3	5.3	38.1	19.7	0.73	160
HB12	50.8	43.2	5.1	0	38.1	24.1	0.90	0.17
HB13	63.5	54.4	5.1	0	38.1	24.1	0.90	0.17
HB14	34.3	27.3	2.9	0	25.4	14.8	0.90	0.14
HB15	63.5	54.4	2.9	0	38.1	16.5	0.90	0.14

## Results and Analysis

### *Screen Porosity*

The nominal (manufacturer reported) openness of a shade is typically a calculated average geometrical openness using tread diameter and threads per inch of the weave. To verify the nominal openness a spectrometer is used, where measured openness is equivalent to the visible specular transmittance of the material. The difference between measured and nominal openness for all shades in this study is shown in Figure 7. The results show a reasonable correlation between measured and nominal openness with a normal distribution of their difference. This means that subsequent thermal performance correlations should be independent of utilizing measured or manufacturer reported openness. This was confirmed and the remainder of analysis in this report is based on correlations utilizing the nominal openness.

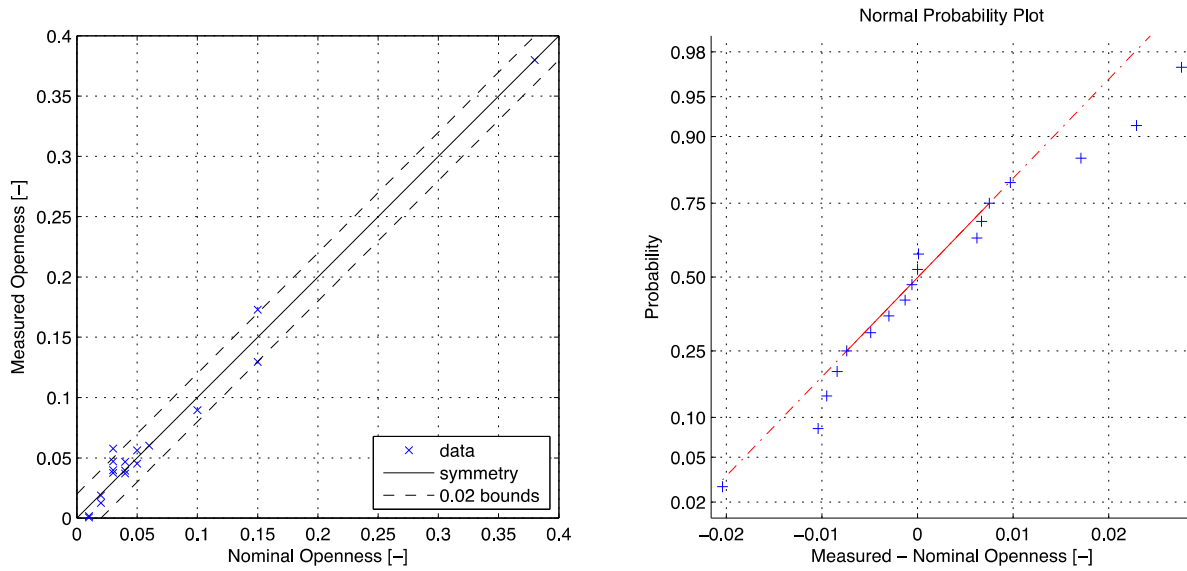


Figure 7. Comparison of measured visible specular transmission and nominal (manufacturer reported) openness

Airflow measurements of several screen materials were made utilizing the methods outlined in ASTM D737 (2008). Results are shown in Table 4 along with the measured layer emissivities. These permeability [ $\text{cm}^3 \text{s}^{-1} \text{cm}^{-2}$ ] measurements were then used to determine the permeability [ $\text{m}^2$ ] as defined by Miguel (1998) and plotted in Figure 8. The measurements performed for the current work show good correlation to the Miguel simplified model. This gives us confidence in the airflow measurements and the applicability of Equation 8 for the shades in this study.

Table 4. Nominal and measured screen properties

<b>ID</b>	<b>Nominal Openness [-]</b>	<b>Emissivity Front [-]</b>	<b>Emissivity Back [-]</b>	<b>Visible Specular Transmittance [-]</b>	<b>Permeability [cm<sup>3</sup> s<sup>-1</sup> cm<sup>-2</sup>]</b>
SE10	0.03	0.851	0.851	0.047	24.0
SE11	0.01	0.895	0.895	0.002	5.2
SE12	0.03	0.839	0.839	0.038	20.8
SE13	0.05	0.864	0.864	0.056	30.1
SE14	0.10	0.825	0.825	0.090	42.4
SE15	0.03	0.930	0.930	0.040	42.9
SE16	0.05	0.880	0.880	0.045	33.7
SE17	0.15	0.748	0.748	0.173	87.9
SE18	0.01	0.917	0.917	0.001	24.3
SE19	0.01	0.813	0.813	0.001	34.5
SE20	0.03	0.833	0.833	0.058	31.6
SE29	0.02	0.854	0.094	0.019	14.7
SE29f	0.02	0.094	0.854	0.019	14.7
SE30	0.38	0.520	0.520	0.380	-
SE31	0.04	0.825	0.114	0.037	22.7
SE31f	0.04	0.114	0.825	0.037	22.7
SE34	0.15	0.731	0.731	0.130	-
SE37	0.06	0.803	0.803	0.060	-
SE41	0.04	0.721	0.109	0.039	-
SE41f	0.04	0.109	0.721	0.039	-
SE42	0.04	0.786	0.272	0.047	-
SE42f	0.04	0.272	0.786	0.047	-
SE46	0.02	0.846	0.057	0.013	-
SE46f	0.02	0.057	0.846	0.013	-
SE54	0.00	0.853	0.848	0.030	-

The emissivities in Table 2 do not always agree between front and back, even for samples without a metallic coating. Depending on the weave patterning, it is common that a two-colored product has different amount of each thread dominating on each side. Asymmetric weave patterns can also give rise to different amounts of self shading surface roughness, which could increase the absorption to a small degree between the two sides. Both sides were measured to capture any such variations, which would allow for instrument noise to cause a difference in value.

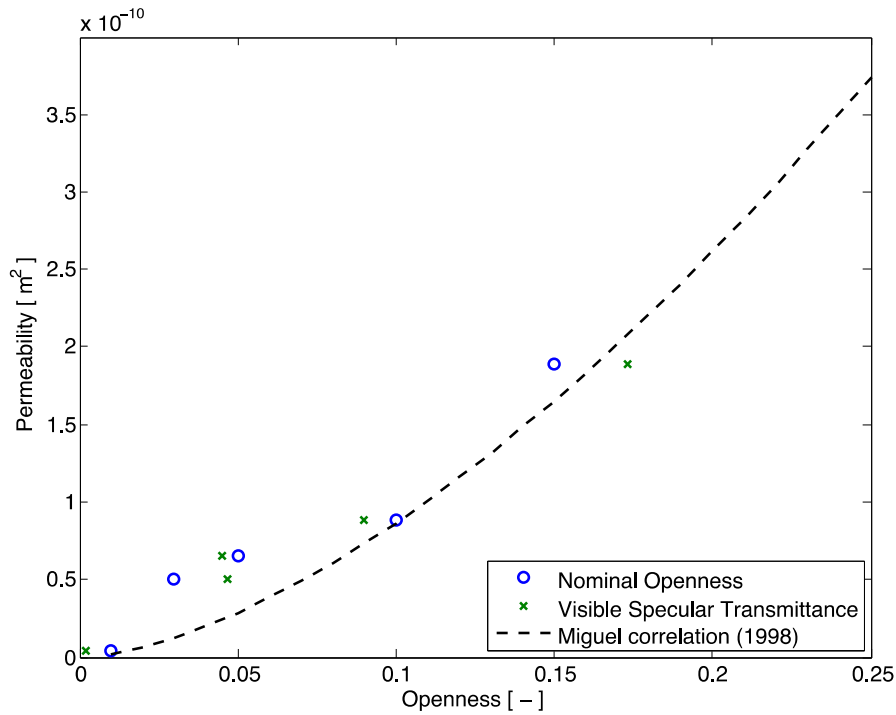


Figure 8. Screen permeability [ $\text{m}^2$ ] as a function of nominal (manufacturer reported) and measured (visible specular transmittance) openness

### **Screen Heat Flux**

The ventilated cavity model from ISO 15099, as implemented in WINDOW, is used to predict thermal transmittance of all measured scenarios. Figure 9 shows a comparison of the measured and simulated heat flux. The WINDOW model appears to provide a reasonable correlation, but with a large,  $\sim 16\%$  on average, systematic over prediction of the thermal transmittance. There is no industry-accepted range for errors or uncertainty in thermal simulation tools or measurements, but within 10% or less is typically considered good agreement for the range of heat flow in this work (NFRC 2010). A revised correlation is thus developed based on the previously presented Darcy-Forchheimer Law correlations from Miguel.



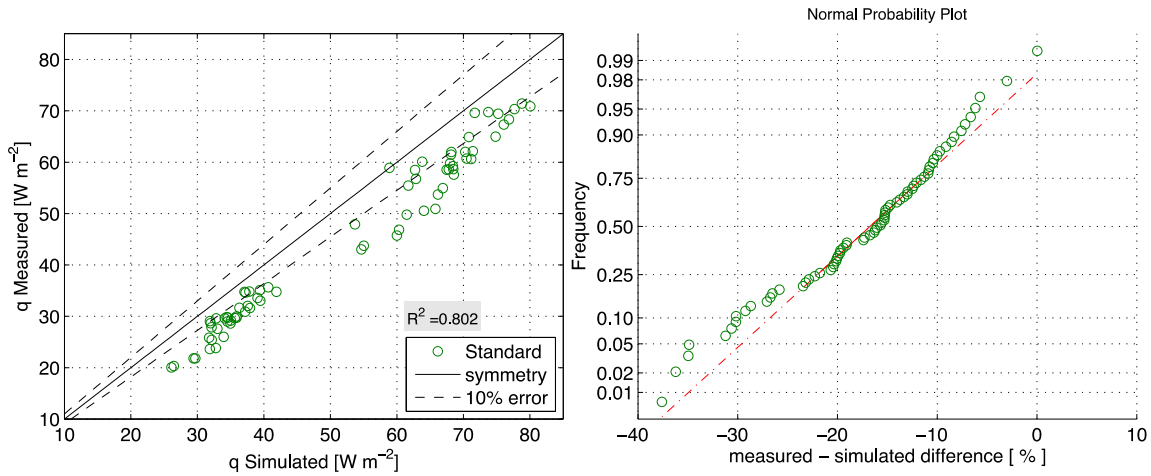


Figure 9. Comparison of WINDOW simulated and measured heat flux of shade systems

The first step to improving the model is to identify the most important physical parameters using an analysis of variance (ANOVA) on the percent difference between the measured and simulated heat flux for the experimental variables listed in Tables 1 and 4. This is performed and presented in Figure 10 with a box plot. The box plot compactly shows key information. The plot identifies the mean through the red center line, the 25% and 75% quartiles through the top and bottom edges of the box, the 95% confidence interval of the mean through the notched lines going out from the mean, the range of included data through the dashed line “whiskers”, and finally it identifies outliers and excludes them from the analysis as shown by the red pluses. A data-point is considered an outlier if it is more than 1.5 times the interquartile range from either quartile.

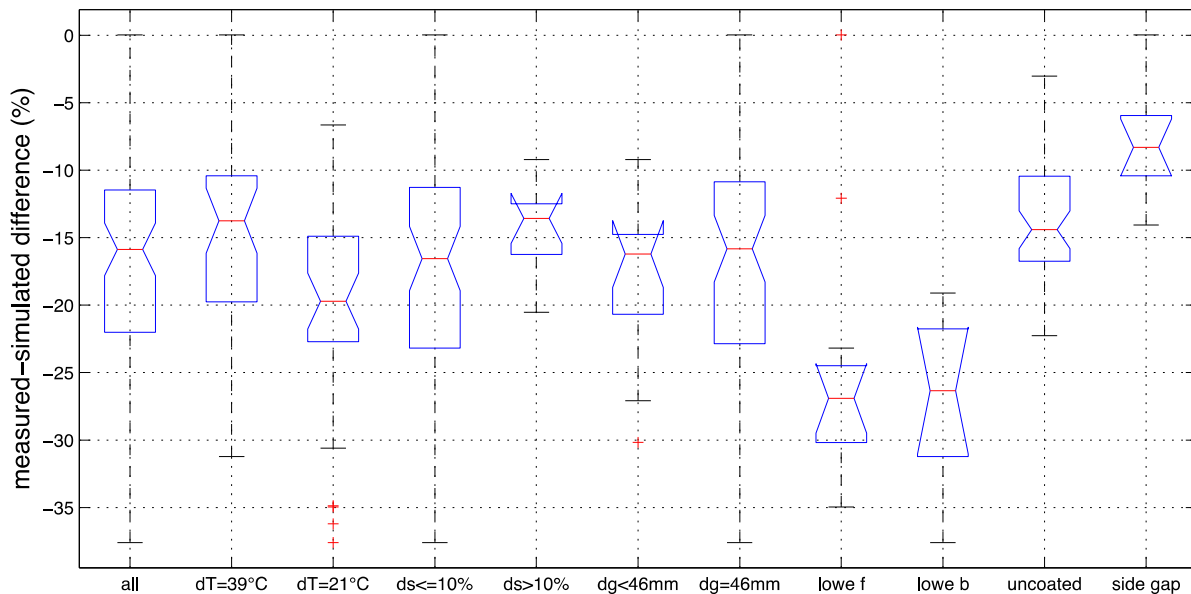


Figure 10. Box plot based of measured - WINDOW simulated difference in heat flux grouped by indoor-outdoor temperature difference ( $dT$ ), openness ( $ds$ ), window-to-shade gap depth ( $dg$ ), the presence of low-e surfaces, and side gaps ( $d_{left}$ ,  $d_{right}$ ).

To improve the simulation correlation, correlation coefficients are proposed to the five ventilated layer opening parameters defined in ISO 15099;  $A_h$ ,  $A_{top}$ ,  $A_{bot}$ ,  $A_l$ , and  $A_r$ . The proposed correlation coefficient for  $A_h$  is of the form presented by Miguel (1998) and shown in Equation 13. This model includes two correlation constants, C1 and C2 that are determined based on regression analysis of the measured dataset. An additional two constants, C3 and C4, are also optimized and used to correlate the to left/right and top/bottom gaps respectively as shown in Equations 14 and 15.

$$\text{Proposed:} \quad A_h = C1 \cdot d_{surface}^{C2} \cdot A_w \quad (13)$$

$$A_{l,r}^* = C3 \cdot A_{l,r} \quad (14)$$

$$A_{t,b}^* = C4 \cdot A_{t,b} \quad (15)$$

The correlation constants C1 - C4 are determined by maximizing the coefficient of determination,  $R^2$ , between the simulated and measured heat flux through the MATLAB constrained nonlinear optimization function `fmincon` with the interior-point algorithm. Utilizing the revised algorithm as described and optimizing the correlation coefficients based on measured data, the accuracy of the simulation increases greatly as shown in Figure 11. The resulting correlation coefficients are listed in Table 5.

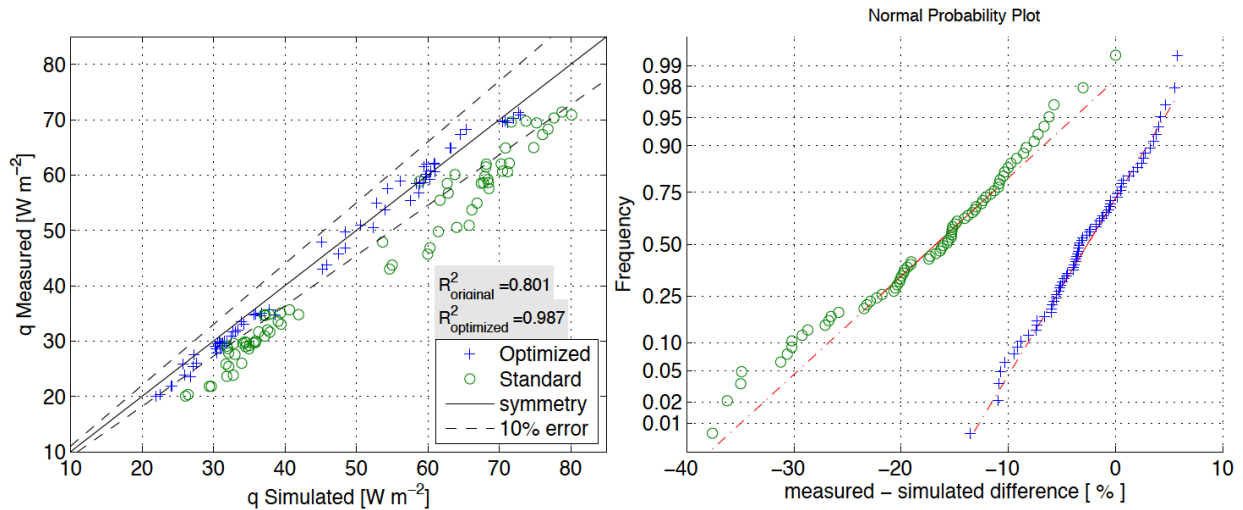


Figure 11. Comparison of WINDOW simulated and measured heat flux of shade systems with proposed correlation constants C1 - C4.

Table 5. Calculated correlation coefficients for proposed WINDOW simulation model of porous surfaces with perimeter gaps

Coefficient	Value
C1	0.078
C2	1.20
C3	1
C4	1

Parameters C3 and C4 resolved to 1, which implies that the poor correlation seen in the old model was not due the perimeter gaps. Correlating nominal openness with the surface openness related factors C1 and C2 proved the primary factors needed to improve the model.

Figure 12 shows the revised mean difference between measured and simulated heat flux for all data falls below perfect symmetry at -3.5 percent, -2.5 percent more than the bias presented in previous validation work with WINDOW for sealed cavities. The most significant error in the model is a function of the warm to cold side temperature difference. The significant variance from low indoor-to-outdoor temperature difference to high temperature difference is presumed to be a divergence of the  $Nu = f(Ra)$  scaling for porous surfaces from those developed for sealed cavities and flat plates that are used in the model.

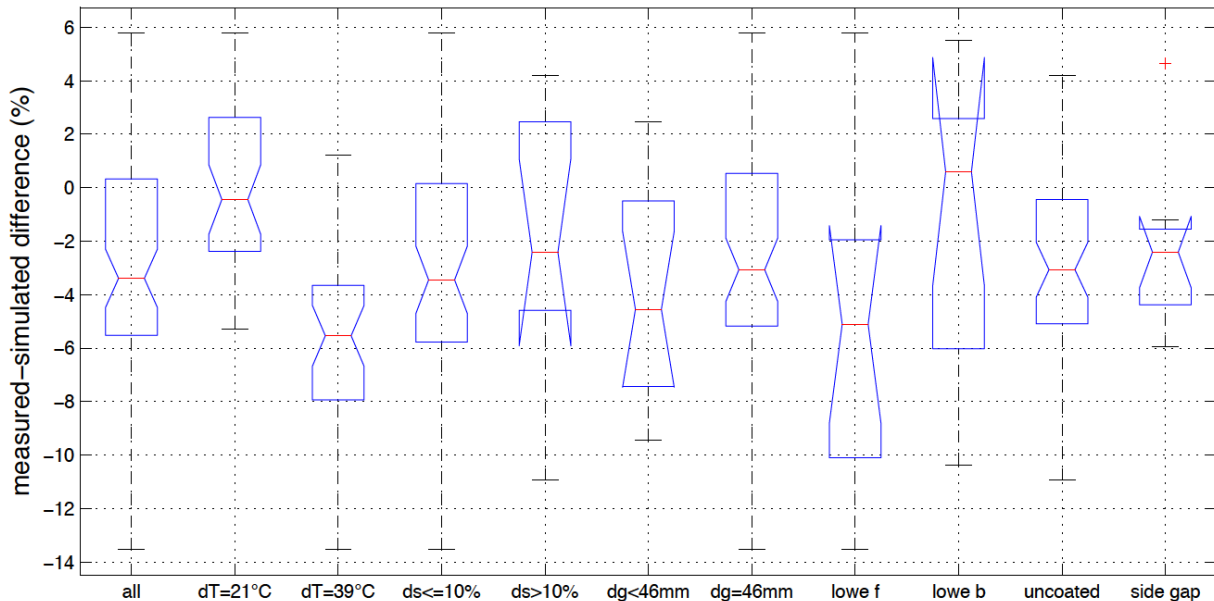


Figure 12. Box plot based of measured – proposed WINDOW simulated difference in heat flux grouped by indoor-outdoor temperature difference ( $dT$ ), openness ( $ds$ ), window-to-shade gap depth ( $dg$ ), the presence of low-e surfaces, and side gaps ( $d_{left}$ ,  $d_{right}$ ).

### Comparison to models from literature

To help understand how the suggested WINDOW model changes compare to existing models, a theoretical combination of clear glass and a “shading system” made of a clear glass with varying openness is modeled. Figure 13 shows the simulated thermal transmittance (U-factor) of a sample 3mm thick shade with optical and physical properties matching those of clear glass. An ideal model should show double-clear performance at zero openness and single-clear performance at openness

of 1. The current WINDOW model is very sensitive to openness up to 0.1 and becomes invalid past this point, as previously shown and expected based on the form of Equations 1-5. The proposed revision to the WINDOW model shows much less sensitivity to openness. This is achieved by significantly reducing openness weighting in the algorithm through C1 and C2. The proposed WINDOW correlations are only correlated to measured results up to  $d_{\text{surface}} \cong 0.38$  so caution should be taken for larger values. The proposed WINDOW model also becomes invalid when  $d_{\text{surface}} \cong 0.75$ .

The authors could find no studies on the direct thermal impacts of screens to window systems as a function of shade openness in the range of 1 to 38 percent. Thermal transmittance comparison is therefore simulated using the Miguel (1998) pressure drop model as described by Laouadi (2009). The Laouadi/Miguel model simulation shows very similar correlation to openness as the proposed WINDOW model. The EN 13125 (2002) model does not correlate well with either model, particularly at high openness.

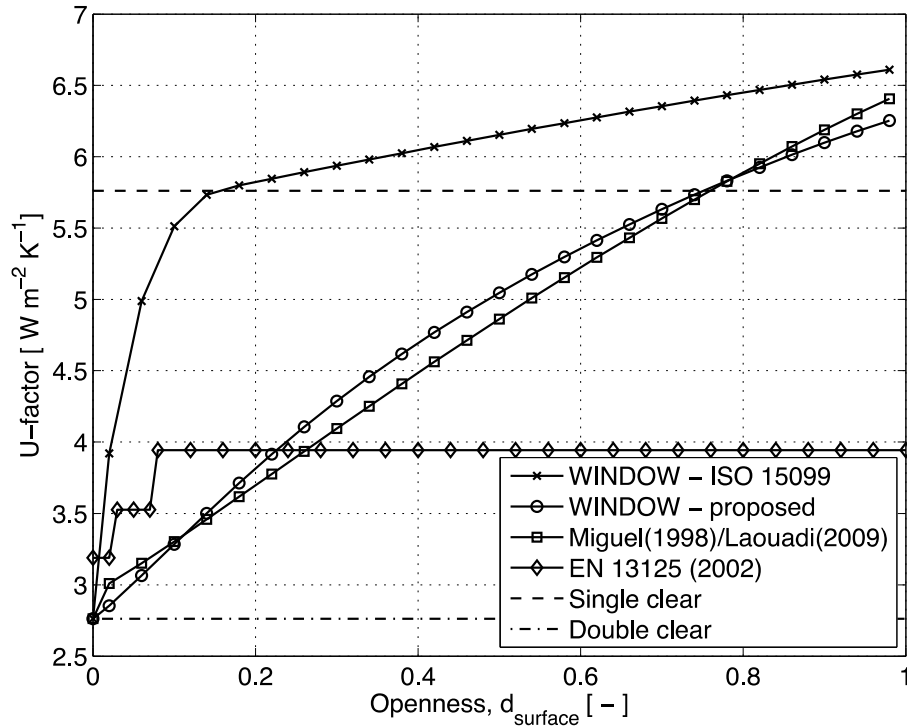


Figure 13. Center-of-glass U-factor as a function of screen openness. WINDOW simulation results compared to literature

### **Horizontal Louvered Blind Heat Flux**

The ventilated cavity model from ISO 15099 as implemented in WINDOW is used to predict heat flux of all measured scenarios. Figure 14 shows a comparison of the measured and simulated heat flux values using a thermal openness of 0.05. ISO 15099 does not provide guidance for an appropriate value of thermal openness and the set point of 0.05 has historically been used by convention in WINDOW for horizontal blinds, without validation. The WINDOW model appears to provide a reasonable correlation, but with a large, ~13% on average, systematic over prediction of the heat flux.

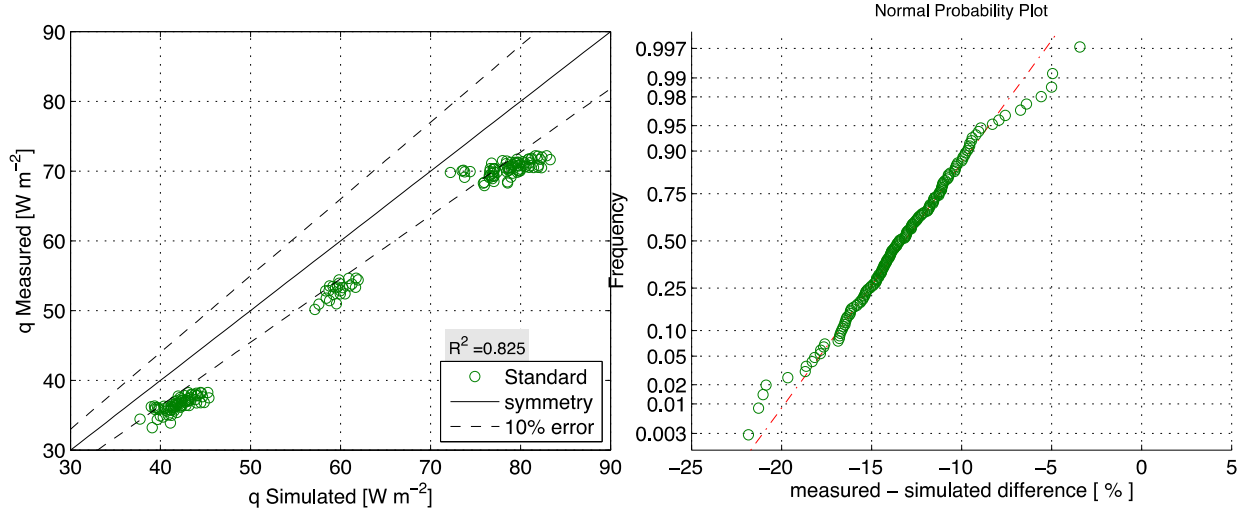


Figure 14. Comparison of WINDOW simulated and measured heat flux of horizontal blind systems

To improve the simulation correlation, correlation coefficients are proposed to the five ventilated layer opening parameters defined in ISO 15099; Ah, Atop, Abot, Al, and Ar. The proposed heat flux model includes parameters for the openness,  $d_{surface}$ , open area,  $A_h$ , tilt,  $\varphi$ , and the layer conductivity,  $k$ . The proposed model for  $A_h$  in Equation 16 is of the logarithmic form presented by Miguel (1998). The openness in Equation 17 is the ratio of slat to open area of the blind layer. This model includes four correlation constants D1, D2, D3, and D4 that are calculated based on the measured dataset according to the optimization procedure previously described.

$$\text{Proposed:} \quad A_h = D1 \cdot [d_{surface} \cdot (\cos \varphi)^{D2}]^{D3} \cdot A_s \quad (16)$$

$$d_{surface} = 1 - \frac{t}{(\cos \varphi) \cdot (p-t)} \quad (17)$$

$$t^* = D4 \cdot w \cdot \cos \varphi \quad (18)$$

$$k^* = d_{surface} \cdot k_c + (1 - d_{surface}) \cdot k_s \quad (19)$$

$$d_{top} = 0 \quad (20)$$

$$d_{left,right} = d_{gap} \quad \text{for outside mount} \quad (21)$$

$$d_{left,right} = 0 \quad \text{for inside mount}$$

$$d_{bottom} = d_{gap} \quad \text{for outside mount} \quad (22)$$

$$d_{bottom} = 0 \quad \text{for inside mount}$$

where  $t^*$  and  $k^*$  are the revised layer thickness and equivalent conductivity and  $k_c$  is the conductivity of the gas between slats at the average blind layer temperature. The calculated

openness by Equation 16 for horizontal blind systems typically results in openness greater than 90%. With the tested inside mount blinds the top, bottom, and side gaps are zero.

Utilizing the revised algorithm as described by Equations 16 – 22, and optimizing the correlation coefficients based on measured data, the accuracy of the simulation increases greatly as shown in Figure 15. The resulting correlation coefficients are listed in Table 6. As shown for porous screens, the current WINDOW model is very sensitive to openness up to 0.1 and becomes invalid past that point. The proposed revisions to WINDOW show much less sensitivity to openness. This is achieved by significantly reducing openness weighting in the algorithm through D1.

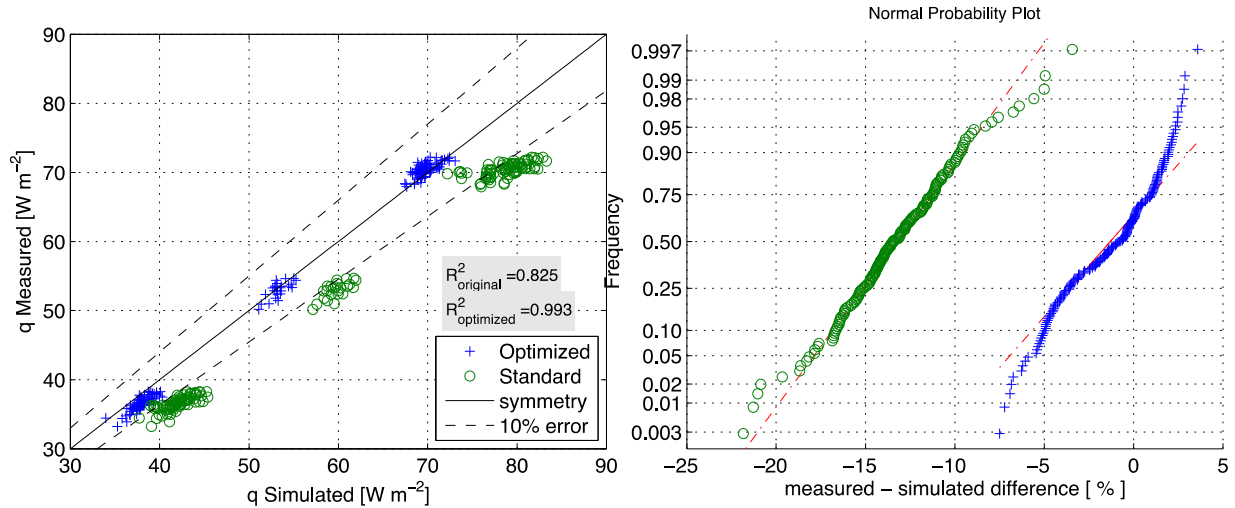


Figure 15. Comparison of proposed WINDOW simulated and measured heat flux of horizontal blind systems

Table 6. Calculated correlation coefficients for proposed WINDOW simulation model for horizontal louvered blinds

Coefficient	Value
D1	0.016
D2	-0.63
D3	0.53
D4	0.043

An ANOVA on the percent difference between the measured and simulated heat flux for the experimental variables listed in Tables 2 and 3 is performed and presented in Figure 16 with a box plot. The figure shows the mean heat flow rate difference for all data falls below perfect symmetry at -1%, similar to the bias presented in previous validation work with WINDOW for sealed cavities. The most significant error in the model is a function of the warm to cold side temperature difference. The significant variance from low indoor to outdoor temperature difference to high temperature difference is presumed to be a divergence of the  $Nu = f(Ra)$  scaling for ventilated surfaces from those developed for sealed cavities and flat plates that are used in the model. This same temperature bias is seen with all ventilated window systems.

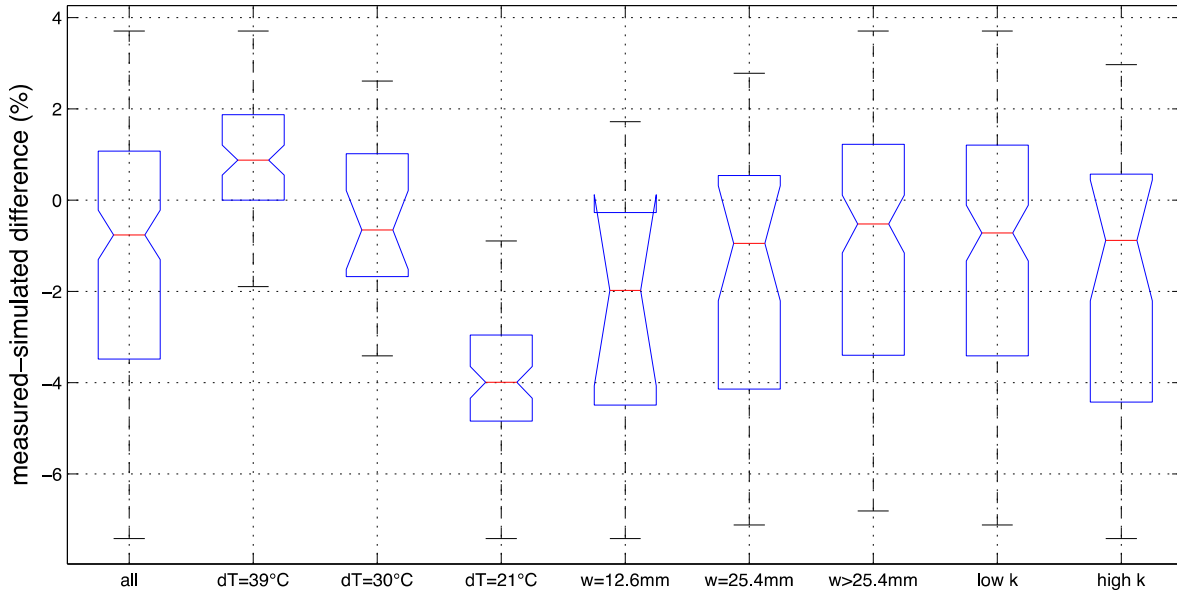


Figure 16. Box plot based of measured – proposed WINDOW simulated difference in heat flux grouped by indoor-outdoor temperature difference (dT), slat width (w), and slat thermal conductivity (k).

Figure 17 shows a second ANOVA but grouped by the blind tilt angle. There is a clear, but relatively small, angle dependent bias. This bias is due to the proposed correlation (Equation 16) assuming symmetry for tilt angles above and below horizontal by utilizing the cosine of the tilt angle. Measurements show the symmetry assumption is invalid. The bias is relatively small, approximately two percent, and is therefore deemed acceptable. A better fit to measured data could be achieved though, if deemed necessary in future work, by considering the full range of blind tilt angles in the correlations.

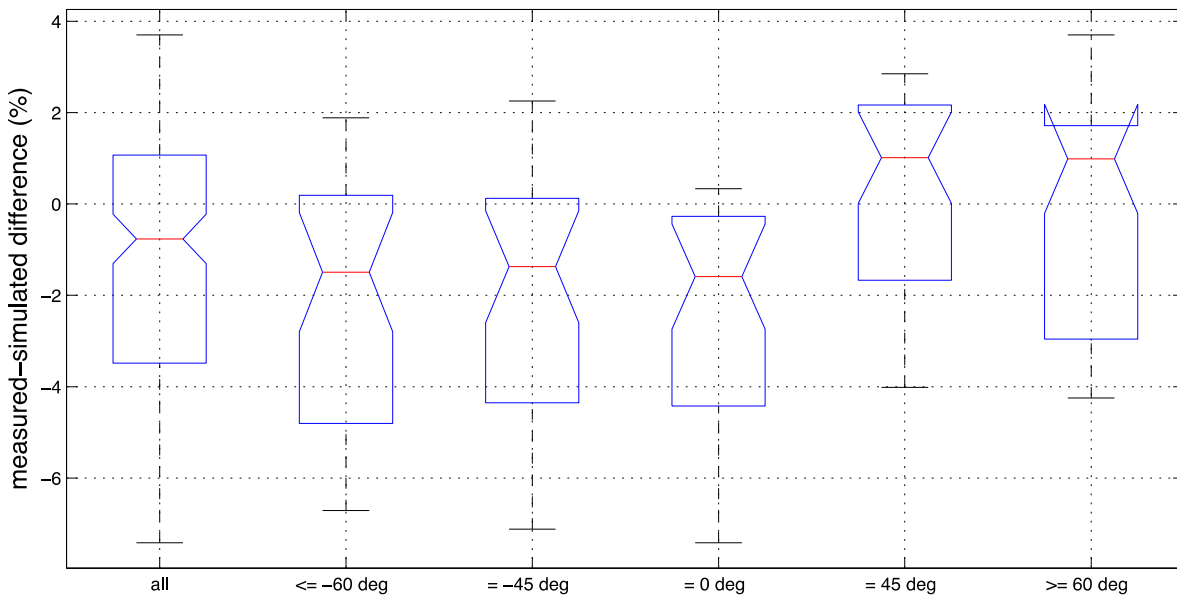


Figure 17. Box plot based of measured – proposed WINDOW simulated difference in heat flux grouped by tilt angle. Negative tilt angles are below horizontal as defined in Figure 13.

### *Comparison to models from literature*

Several authors have performed CFD analysis and simplified model development of systems with internal horizontal blinds. A comparison of the U-factor ratio of a blind system compared to a double-pane clear glass base window for several models from literature is shown in Figure 18 over a range of blind tilt angles. The results shown are for ASHRAE summer boundary conditions of  $T_c = 32\text{ }^\circ\text{C}$ ,  $T_w = 24\text{ }^\circ\text{C}$  and a combined outdoor convective coefficient of  $16.77\text{ Wm}^{-2}\text{K}^{-1}$ . Base window performance under these boundary conditions is  $U = 2.78\text{ Wm}^{-2}\text{K}^{-1}$  (WINDOW simulation). Blind configuration is fixed at a  $w = 25.4\text{ mm}$ ,  $k = 123\text{ Wm}^{-1}\text{K}^{-1}$ ,  $p = 22.28\text{ mm}$ ,  $t = 0.16\text{ mm}$ ,  $r = 1\text{ mm}$ , and  $d_{\text{gap}} = 27.5\text{ mm}$ . Slat emissivity is indicated in the legend. It's not physically possible for blind systems to tilt a full 90 degrees because pitch is typically less than slat width. Additionally, slat curvature and internal limits set by the blind manufacturer prevent full rotation. The WINDOW model sets the maximum tilt to smallest angle where  $d_{\text{surface}} = 0$  in Equation 14. The maximum tilt angle for the slat geometry used in Figure 18 is approximately 88 degrees.

Exterior mount blind configurations show good agreement between the proposed WINDOW model and previous studies by Shahid (2005), Naylor (2006), and Laouadi (2009). Agreement is also good with EN 13125 for fully-tilted high-emissivity slats. The proposed WINDOW calibration is to real horizontal blind systems with an inside mount configuration that includes top and bottom rails, rather than the simplified flat plate model more representative of an external mounting used for all other models from literature. The curves for the proposed WINDOW model assuming an internal mount show improved performance of  $U/U_{\text{base}} \cong 0.08$  when compared to external mounting.



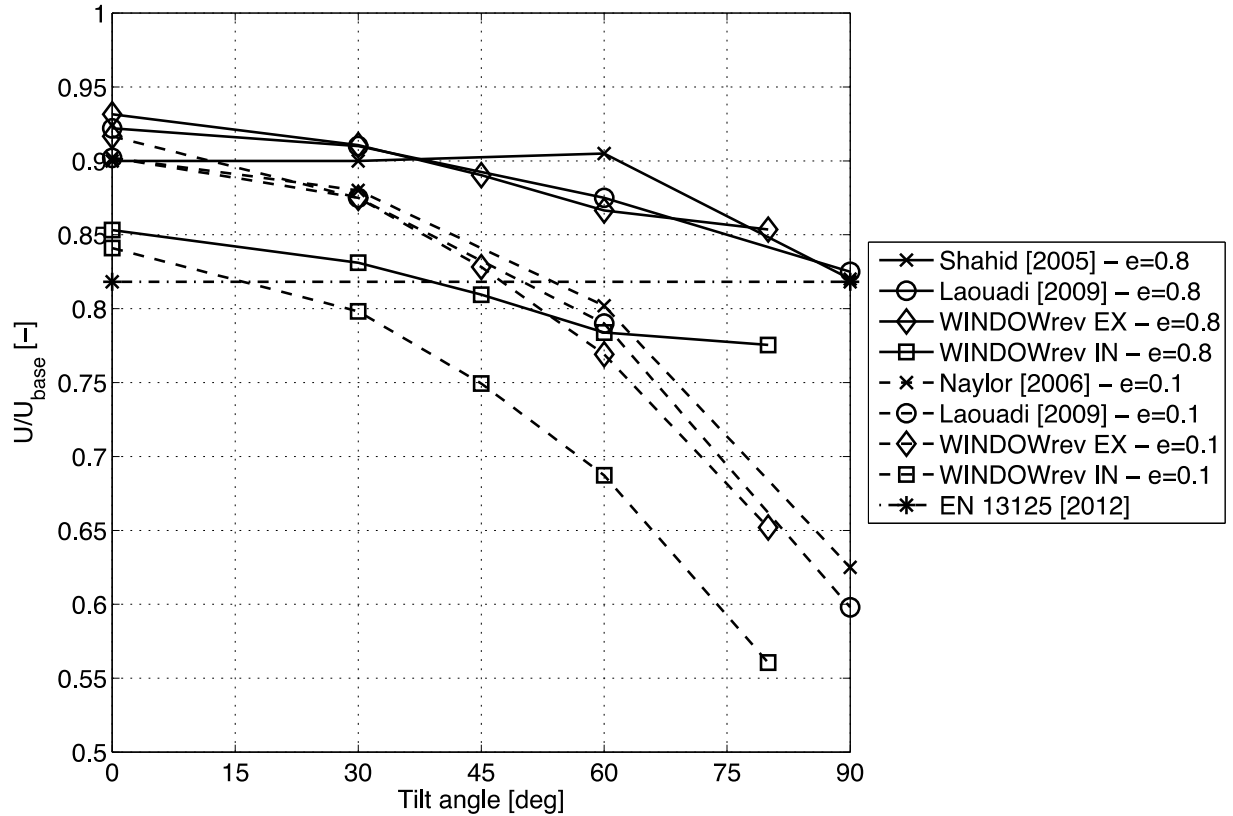


Figure 18. Comparison of thermal transmittance calculated with proposed WINDOW simulation and literature.  $e$  = slat emissivity, IN = inside mount, EX = outside mount

## Conclusions

The ISO 15099 model for ventilated cavities through perforated surfaces with connection to the indoor environment, such as solar screens, is shown to have poor accuracy in predicting heat flux as it is currently implemented in the WINDOW software program. A revision to that implementation with greater accuracy through correlation coefficients is therefore proposed and demonstrated. The proposed correlation changes the mean error between measured and simulated heat flux for the configurations measured from 16% to 3.5%. It also reduces the interquartile range of errors from 11% to 6%. The proposed correlation coefficients apply for materials bounded by the ranges tested: 1 – 38 percent openness, glass to screen gap dimensions of 18 - 46mm, and indoor to outdoor temperature differences of 21 – 39°C. The model shows significant bias in predicting performance based on the indoor to outdoor temperature difference. The bias is presumed to be a divergence of the  $Nu = f(Ra)$  scaling for porous surfaces from those developed for sealed cavities and/or flat plates that are used in the model. Further investigation into the convective heat transfer coefficient as a function of temperature is therefore recommended for future work. The vast majority of solar screens on the market are from 1 to 10 percent openness. The proposed WINDOW model shows a good correlation for this range. Additional work should be done to confirm the validity of the proposed correlations for openness greater than about 15 percent.

The ISO 15099 model for interior mounted horizontal blinds is also shown to have poor accuracy in predicting heat flux as it is currently implemented in the WINDOW software program. A revision to that implementation with greater accuracy is therefore proposed and demonstrated.

The proposed correlation changes the mean error between measured and simulated heat flux for the configurations measured from 13% to 1% while maintaining the interquartile range of errors at 5%. The proposed model is based on openness correlations from Miguel along with several additional geometry based factors. Correlation coefficients that fit the model to measured data are determined by optimizing the coefficient of determination between measured and simulated heat flux for the 176 configurations of horizontal blinds examined. The proposed correlation coefficients apply for horizontal blinds bounded by the range of properties tested: 12 – 65 mm slat width, glass to slat tip dimensions of 18 – 110 mm, and indoor to outdoor temperature differences of 21 – 39°C. Outside of these ranges the model has not been validated, but does agree well with literature in cases where comparisons are possible, such as temperature differences of 8°C.

## References

- ASTM International. (2015). C1371-15 Standard Test Method for Determination of Emittance of Materials Near Room Temperature Using Portable Emissometers. West Conshohocken, Pa.
- ASTM International. (2014). C1199-14 Standard Test Method for Measuring the Steady-State Thermal Transmittance of Fenestration Systems Using Hot Box Methods. West Conshohocken, Pa.
- ASTM International (2008). D737-04 Standard Test Method for Air Permeability of Textile Fabrics. West Conshohocken, Pa.
- Bejan, A. (2004). Convection Heat Transfer. 3rd ed. John Wiley & Sons, Inc.
- Brunger, A., Dubrous, F. M., & Harrison, S. (1999). Measurement of the solar heat gain coefficient and U value of windows with insect screens. ASHRAE Transactions, 105.
- Carlos, J. S., & Corvacho, H. (2014). Evaluation of the thermal performance indices of a ventilated double window through experimental and analytical procedures:  $U_w$ -values. Renewable Energy, 63, 747–754.
- Carlos, J. S., Corvacho, H., Silva, P. D., & Castro-Gomes, J. P. (2011). Modelling and simulation of a ventilated double window. Applied Thermal Engineering, 31(1), 93–102.
- Clark, J., Peeters, L., & Novoselac, A. (2013). Experimental study of convective heat transfer from windows with Venetian blinds. Building and Environment, 59, 690–700.
- Collins, M. (2004). Convective heat transfer coefficients from an internal window surface and adjacent sunlit Venetian blind. Energy and Buildings, 36(3), 309–318.
- Collins, M. R., & Harrison, S. J. (1999). Calorimetric Measurement of the Inward- Flowing Fraction of Absorbed Solar Radiation in Venetian Blinds. ASHRAE Transactions, 15(2).
- Collins, M. R., & Harrison, S. J. (2004a). Calorimetric analysis of the solar and thermal performance of windows with interior louvered blinds. ASHRAE Transactions, 110 PART 1, 474–485.

- Collins, M. R., & Harrison, S. J. (2004b). Estimating the solar heat and thermal gain from a window with an interior venetian blind. *ASHRAE Transactions*, 110 PART 1, 486–500.
- Collins, M.R., Tasnim, S., & Wright, J. (2009). Numerical analysis of convective heat transfer in fenestration with between-the-glass louvered shades. *Building and Environment*, 44(10), 2185–2192.
- Cuevas, C., Fissore, A., & Fonseca, N. (2010). Natural convection at an indoor glazing surface with different window blinds. *Energy and Buildings*, 42(10), 1685–1691.
- Devices and S. Co., (1981). Use of emissometer for semi-transparent materials measurements. Tech. rep., D&S Technical Note 81-1.
- van Dijk, D., & Oversloot, H. (2003). WIS, the European tool to calculate thermal and solar properties of windows and window components. *Proceedings of Building Simulation*, 259–266.
- Fang, X. (2001). Study of the U-factor of a window with a cloth curtain. *Applied Thermal Engineering*, 21(5), 549–558.
- Garnet, J. M., Fraser, R. A., Sullivan, H. F., & Wright, J. L. (1995). Effect of Internal Blinds on Window Center-Glass U-Values. In *Window Innovations '95* (pp. 273–279). Toronto, Canada.
- Grasso, M. M., & Buchanan, D. R. (1979). Roller Shade System Effectiveness In Space Heating Energy Conservation. *ASHRAE Transactions*, 85(2520).
- Grasso, M., Hunn, B., & Briones, R. (1990). Effect of Textile Characteristics on the Thermal Transmittance of Interior Shading. *ASHRAE Transactions*, 96(1).
- Harrison, S. J., & van Wonderen, S. J. (1998). Evaluation of solar heat gain coefficient for solar-control glazings and shading devices. *ASHRAE Transactions*, 104(Pt 1B), 1051–1062.
- International Organization for Standardization 15099. (2003). *Thermal Performance of Windows, Doors, and Shading Devices—Detailed Calculations*. Geneva, Switzerland.
- International Organization for Standardization 12567-1. (2010). *Thermal performance of windows and doors -- Determination of thermal transmittance by the hot-box method -- Part 1: Complete windows and doors*. Geneva, Switzerland.
- Ismail, K. a R., & Henríquez, J. R. (2005). Two-dimensional model for the double glass naturally ventilated window. *International Journal of Heat and Mass Transfer*, 48(3-4), 461–475.
- Kotey, N. A., Wright, J. L., Barnaby, C. S., & Collins, M. R. (2009). Solar gain through windows with shading devices: Simulation versus measurement. *ASHRAE Transactions*, 115 PART 2, 18–30.

- Laouadi, A. (2009). Thermal performance modeling of complex fenestration systems. *Journal of Building Performance Simulation*, 2(3), 189–207.
- Marjanovic, L., Cook, M., Hanby, V., & Rees, S. (2005). CFD Modeling of Convective Heat Transfer From a Window with Adjacent Venetian Blinds. In *Building Simulation* (pp. 709–716).
- Miguel, A. F. (1998). Airflow through porous screens: From theory to practical considerations. *Energy and Buildings*, 28(1), 63–69.
- National Fenestration Rating Council. (2010). NFRC-100-2010E0A1. Procedure for Determining Fenestration Product U-factors.
- Naylor, D., & Collins, M. (2005). Value of a Window With a Between-Panes Blind. *Numerical Heat Transfer, Part A: Applications*, 47(3), 233–250.
- Naylor, D., Duarte, N., Machin, a. D., Phillips, J., Oosthuizen, P. H., & Harrison, S. J. (2002a). An Interferometric Study of Free Convection at a Window Glazing with a Heated Venetian Blind. *Journal of Heat Transfer*, 124(4), 598.
- Naylor, D., Duarte, N., Machin, a. D., Phillips, J., Oosthuizen, P. H., & Harrison, S. J. (2002b). Visualization of Convection at an Indoor Window Glazing With a Venetian Blind. *Journal of Heat Transfer*, 124(4), 598.
- Naylor, D., & Shahid, H. (2006). A simplified method for modeling the effect of blinds on window thermal performance. *International Journal of Energy Research*, 471–488.
- NF EN 13125. (2012). Shutters and Blinds - Additional thermal resistance - Allocation of a class of air permeability to a product. La Plaine Saint-Denis Cedex.
- Norris, N. (2009). Numerical Analysis of Natural Convection Heat Transfer for Windows with Porous Screening Material. Thesis, University of Waterloo.
- Oosthuizen, P. H., Sun, L., Harrison, S. J., Naylor, D., & Collins, M. (2005). The Effect of Coverings on Heat Transfer from a Window to a Room. *Heat Transfer Engineering*, 26(5), 47–65.
- Roeleveld, D., Naylor, D., & Oosthuizen, P. (2010). A simplified model of heat transfer at an indoor window glazing surface with a Venetian blind. *Journal of Building Performance Simulation*, 3(2), 121–128.
- Shahid, H., & Naylor, D. (2005). Energy performance assessment of a window with a horizontal Venetian blind. *Energy and Buildings*, 37(8), 836–843.
- Tait, D. B. (2006). Solar Heat Gain for Glazings with Indoor Window Attachment Products. *ASHRAE Transactions*, 112.
- Tanimoto, J., & Kimura, K. (1997). Simulation study on an air flow window system with an integrated roll screen. *Energy and Buildings*, 26(3), 317–325.

- Tarcog: Mathematical Models for calculation of thermal performance of glazing systems with or without shading Devices. (2006). Carli, Inc.
- Wang, D., Liu, Y., Wang, Y., Zhang, Q., & Liu, J. (2015). Theoretical and experimental research on the additional thermal resistance of a built-in curtain on a glazed window. *Energy and Buildings*, 88, 68–77.
- Wright, J. L. (2008). Calculating Center-Glass Performance Indices of Glazing Systems with Shading Devices. *ASHRAE Transactions*, 114(2), 199–209.
- Wright, J. L., Collins, M. R., & Huang, N. (2008). Thermal resistance of a window with an enclosed venetian blind: A simplified model. *ASHRAE Transactions*, 114 PART 1, 471–482.
- Yahoda, D. S., Wright, J. L., D, P., & Eng, P. (2004). Effective Longwave Radiative Properties of a Venetian Blind Layer. *ASHRAE Transactions*, 110.
- Ye, P., Harrison, S. J., & Oosthuizen, P. H. (1999). Convective Heat Transfer from a Window with a Venetian Blind : Detailed Modeling. *ASHRAE Transactions*, 15.